European Review for Medical and Pharmacological Sciences 2019; 23: 877-884

Effect of endostatin on proliferation, invasion and epithelial-mesenchymal transition of basal cell carcinoma cell A431

P. HU[1], L. MA[1], Z.-Q. WU[1], G.-Y. ZHENG[1], J.-T. LI[2]

[1]Department of Plastic Surgery, Henan Province Luoyang Orthopedic Thraumatological Hospital (Henan Provincal Orthopedic Hospital), Luoyang, Henan, China.
[2]Laboratory of Molecular Biology, Henan Province Luoyang Orthopedic Thraumatological Hospital (Henan Provincal Orthopedic Hospital), Luoyang, Henan, China

Abstract. – OBJECTIVE: To investigate the effect of endostatin on the proliferation, invasion and epithelial-mesenchymal transition (EMT) of human basal cell carcinoma (BCC) cells (A431).

PATIENTS AND METHODS: CCK-8 assay and transwell chamber assay were performed to detect cell proliferation and invasion abilities, respectively. Western blot was performed for the detection of the expressions of EMT-related proteins levels. The therapeutic effect of endostatin on tumor formation was tested using a mouse xenograft model.

RESULTS: After endostatin treatment, transwell assay showed that the number of invasive cells in the observation group and control group were (38.25±8.13) and (98.25±9.14), respectively; the relative expression level of E-cadherin protein in the observation group was (0.34±0.03), which was significantly higher than that in the control group (0.14±0.01); the relative expression levels of N-cadherin protein in the observation group was (0.18±0.05), which was significantly lower than that in the control group (0.43±0.03), (all $p<0.05$).

CONCLUSIONS: The expression levels of Vimentin and Fibronectin proteins were significantly lower, while the expression levels of α-smooth muscle Actin (α-SMA) were significantly higher in the observation group than those in the control group. Treatment with endostatin significantly inhibited tumor growth in the mouse xenograft model. Therefore, endostatin can inhibit the proliferation, invasion and EMT in BCC.

Key Words:
Endostatin, Basal cell carcinoma cell, Proliferation, Invasion, Epithelial-mesenchymal transition.

Introduction

Basal cell carcinoma (BCC) originates from the basal cells of the skin or its accessory organs, so BCC is also called basal cell epithelial tumor[1]. BCC accounts for about 60% of malignant tumors in the skin that occurs in light-colored races. BCC mainly affects men and elderly patients, and the affected regions are mainly face, neck and hand skin[2]. Studies have shown that ultraviolet (UV) exposure is closely related to the pathogenesis of BCC that may also be induced by other non-environmental factors such as ionizing radiation, dust and high-fat diet[3]. In addition, HPV infection may also induce the occurrence of BCC4. Studies have shown that mutations in oncogenes and tumor suppressor genes (such as p53 and PTCH) frequently occur in BBC patients[5]. BCC has the potential to differentiate in multiple directions, with a total of nine histological types such as superficial and pigmented types[6]. At present, surgical resection is the first choice for the treatment of BCC, but it will affect the patient's appearance and related functions. Radiotherapy and chemotherapy have certain toxic and side effects, which are not conducive to the long-term survival of patients[7].

Endostatin is an inhibitor of angiogenesis that inhibits tumor neovascularization and cell proliferation, and induces apoptosis[8]. Various studies have shown that it has an inhibitory effect on lung cancer, rectal cancer and other cancers, but its role in BCC has not been clarified. This work aimed to reveal the function of endostatin in BCC by investigating its effects on the proliferation, migration, invasion and epithelial-mesenchymal transition (EMT) of A431 cells, to provide a new theoretical basis for the treatment of BCC.

Materials and Methods

Materials and Reagents

Human BCC cell strain A431 (Jennio Biotech Co., Ltd., Guangzhou, China); fetal bovine serum

Corresponding Author: Jitian Li, MD; e-mail: lyhsh@126.com

(FBS) and Roswell Park Memorial Institute-1640 culture medium (RPMI-1640; HyClone, South Logan, UT, USA); endothelial cell inhibitant endostatin (Shenzhen Biotechnology Co., Ltd., Guangzhou, China); TRIzol reagent, radioimmunoprecipitation assay (RIPA) lysate and sodium dodecyl sulphate-polyacrylamide gel electrophoresis (SDS-PAGE) buffer solution (Shanghai Yisheng Biotechnology Co., Ltd, Shanghai, China); rabbit anti-human E-cadherin (Cat nos. ABP51220, Abbkine, Wuhan, China)/N-cadherin (Cat no. ABP51903, Abbkine, Wuhan, China)/vimentin (Cat no. ABP50223, Abbkine, Wuhan, China)/fibronectin (Cat no. ABM40137, Abbkine, Wuhan, China)/α-smooth muscle Actin (α-SMA) (Cat no. LS-C169737, LSBio, Seattle, WA, USA) polyclonal antibody, rabbit anti-human GAPDH (Cat no. ABP50152, Abbkine, Wuhan, China) polyclonal antibody and horseradish peroxidase labeled goat anti-rabbit secondary antibody (Cat nos. A12004-1, EpiGentek, Farmingdale, NY, USA); Cell Counting Kit-8 (CCK-8) cell proliferation assay kit (Wuhan Biotechnology Co., Ltd., Wuhan, China); transwell chamber and Matrigel (Shanghai Ziqi Biotechnology Co., Ltd, Shanghai, China).

CCK-8 Assay to Detect the Effects of Endostatin on A431 Cell Proliferation

A431 cells were cultured in RPMI-1640 complete medium with 10% fetal bovine serum (FBS) in an incubator at 37°C, 5% CO_2 and humidity of 60%. Cells were harvested at logarithmic growth phase (fusion rate was 90%) to prepare single cells suspensions (1×105/ml). Cells were transferred to a 96-well plate with 1×104 cells/100 μl/well. Endostatin was added at doses of 0 (control), 20, 40, 80 and 160 μl/mg. Three replicates were set for each dose. 10 μl of CCK-8 solution was added 24 h, 48 h and 72 h later. Cells were cultured for an additional 3 hours and the absorbance at 450 nm was measured using a microplate reader. The proliferation inhibition rate = 1 - (endostatin well)/(control well).

CCK-8 Assay of Cell Viability

Based on the results of inhibitory concentration (IC) 50 of A431 cells after endostatin treatment, the action time and concentration of endostatin in the subsequent experiment were determined. The observation group was treated with endostatin, while the control group was treated with an equal amount of RPMI-1640 medium. CCK-8 was used to detect cell viability after cell culture for 12 h, 24 h, 48 h, 72 h, and 96 h. The specific procedures were the same as described in 2.1. Three replicates were set for each sample. Detection was repeated 3 times for each well.

Transwell Invasion Experiment

Trypsin-digested each group of cells was starved for 12 h and single cell suspensions (1×105/ml) were prepared with the serum-free RPMI-1640 medium. The cell suspensions were transferred to the upper chamber of a 24-well transwell with 100 μl/well. 600 μl 1640 medium supplemented with 10% fetal bovine serum was added into the lower chamber. Cells were incubated at 37°C and 5% CO2 for 24 h. After that, polycarbonate membrane was fixed with 5% glutaraldehyde for 10 min, followed by crystal violet staining for 10 min. After being washed with phosphate-buffered saline (PBS) two times, a sterile cotton swab was used to gently wipe off Matrigel. Five visual fields were randomly selected under the microscope (100 times) to count invading cells. The 8 μm chamber was used in the invasive experiment, and the matrix adhesive was Matrigel of BD Biosciences (Franklin Lakes, NJ, USA).

Western Blot

Cells were lysed with RIPA lysate, and the concentration of total protein was determined using the bicinchoninic acid (BCA) method. After denaturing, 10% SDS-PAGE electrophoresis was performed, followed by gel transfer to polyvinylidene difluoride membrane. After that, membranes were blocked in 5% skim milk for 2 h at room temperature. Rabbit anti-human E-cadherin/N-cadherin/vimentin/fibronectin/α-SMA polyclonal antibody was added at a ratio of 1:1000, rabbit anti-human endogenous control GAPDH polyclonal antibody was added at a ratio of 1:3000. After incubation at room temperature for 2 h, membranes were washed with Tris-Buffered Saline and Tween (TBST) and labeled horseradish peroxidase goat anti-rabbit secondary antibody was added at a ratio of 1:9000, followed by incubation at room temperature for 1 h. After washing with TBST 5 times, signals were developed and the gray value of each protein band was analyzed using Quantity One software (Bio-Rad, Hercules, CA, USA). The relative expression level of protein = the gray value of the target protein band/the gray value of GAPDH protein band. Repeating 3 rounds of experiments, each round of experiments was repeated 3 times for each sample.

Table I. Proliferation inhibition rate of A431 treated with different concentrations of endostatin at different times (%).

	0 μl/mg endostatin	20 μl/mg endostatin	40 μl/mg endostatin	80 μl/mg endostatin	160 μl/mg endostatin	F	*p*
24h	(2.24±1.01)*	(12.43±1.45)*	(21.41±2.12)*	(34.21±3.58)*	(46.29±4.16)*	18.58	0.00
48h	(11.53±1.92)*#	(19.62±1.23)*#	(33.71±2.11)*#	(44.68±3.94)*#	(59.31±4.91)*#	17.55	0.00
72h	(16.42±1.93)*#	(29.91±2.19)*#	(46.72±2.98)*#	(61.93±4.01)*#	(85.92±5.93)*#	12.90	0.01
F	16.61	12.62	26.97	41.67	66.71		
p	0.00	0.00	0.00	0.00	0.00		

Note: *: the treatment time is the same, compared with the previous low concentration gradient, $p<0.05$. #: the concentration gradient is the same, compared with the previous treatment time, $p<0.05$.

Nude Mouse Xenograft Model

Fifteen Specific Pathogen Free (SPF) female nude mice (4-6 weeks old) were raised in SPF animal rooms. A431 cells were harvested at logarithmic growth phase and were digested with 0.25% trypsin to prepare single cell suspensions. 0.3 mL of the cell suspension (1.0×107/ml) was subcutaneously injected into the left side of the nude mouse. On the 10th day when tumor diameter reached 6 mm, mice were randomly divided into control group (administered with the same amount of normal saline), ES1 group (administered with the 5 mg/kg endostatin) and ES2 group (administered with the 15 mg/kg endostatin). Endostatin treatment was performed for 14 days9,10 and tumors were measured every two days to calculate tumor volume according to the following formula: tumor volume = long diameter×short diameter2/2. Tumor growth curves were plotted. Animals were sacrificed on the 15th day after treatment. Tumors were weighed and tumor inhibition rate (TIR) was calculated: TIR = (mean tumor volume of control group - mean tumor volume of endostatin group)/mean tumor volume of control group x 100%. This study was approved by the Ethics Committee of Henan Luoyang Orthopaedic Hospital (Henan Orthopaedics Hospital).

Statistical Analysis

SPSS 20.0 (Asia Analytics Formerly SPSS China) software statistical package was used for the analysis of all data. Measurement data were expressed as mean ± standard deviation ($\bar{x} \pm s$), and the t-test was used for comparisons between the two groups. The comparisons among multiple groups were analyzed by univariate factor ANOVA, followed by LSD test. The repeated measures analysis of variance was used for comparisons between different time points in the same group. GraphPad Prism 5 (Shanghai Cabot Information Technology Co., Ltd., Shanghai, China) was used to calculate IC50. The significance level is $\alpha=0.05$.

Results

Determination of IC 50 of A431 Cells After Endostatin Treatment

After A431 cells were treated with different dosages of endostatin for 24 h, 48 h and 72 h, cell proliferation rate was measured by the CCK-8 assay. It was found that endostatin inhibited cell proliferation in a time- and dose-dependent manner (see Table I and Figure 1 for details). The IC50 values at 24 h, 48 h and 72 h were 168.31 μg/ml, 93.44 μg/ml and 53.33 μg/ml, respectively. Treatment with endostatin at 40 μl/mg for 72 h was used for subsequent experiments.

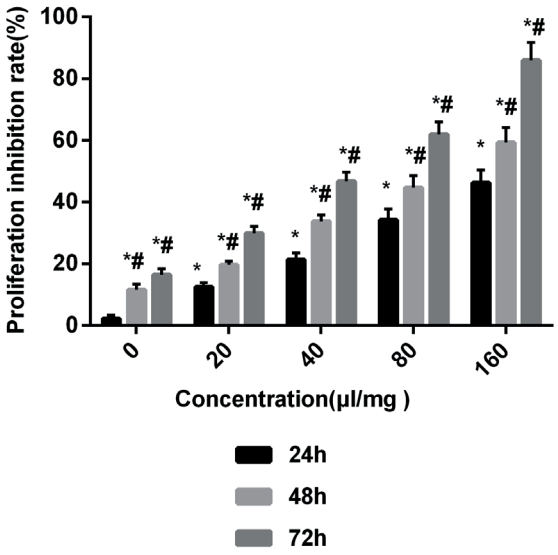

Figure 1. Endostatin on A431 proliferation inhibition rate. After A431 was treated with endostatin with different concentrations for 24 h, 48 h and 72 h, the cell proliferation inhibition rate was detected by CCK8 assay. It was observed that endostatin inhibited cancer cell proliferation in a dose and time-dependent manner. Note: *: compared with the previous low concentration gradient at the same time point, $p<0.05$. #: compared with the previous treatment time at the same concentration of endostatin, $p<0.05$.

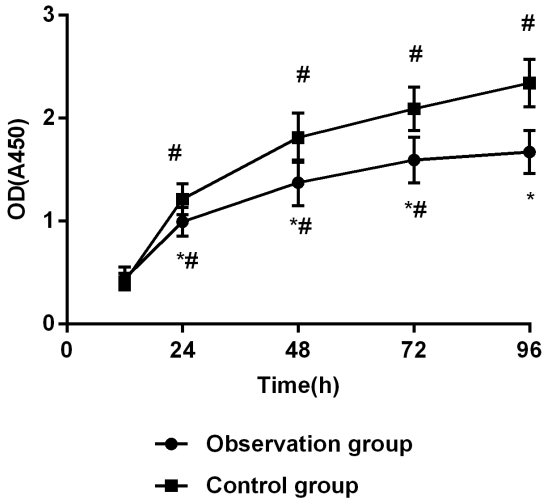

Figure 2. Effect of endostatin on proliferation ability of A431 cells. There was no significant difference in OD values (450) at 24 h between the observation group and the control group (p>0.05). After 24 h, at each time point, OD values of the observation group were significantly lower than those of the control group (p<0.05) at each time point; the OD values (450) in both groups were increased with prolonged time. Note: *: compared with the control group at the same time point, p<0.05. #: compared with the previous time point in the same group, p<0.05.

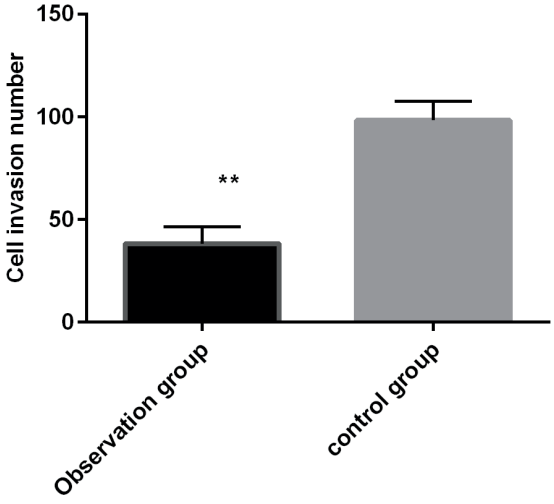

Figure 3. Effect of endostatin on invasion ability of A431 cells. A431 cells were treated with 40 μl/mg of endostatin for 72 h in experimental group, and the equal amount of culture medium was used in the control group. The transwell invasion assay results showed that the number of invasive cells in the observation group and control group were (38.25±8.13) and (98.25±9.14), respectively, and the number of invading cells in the observation group was significantly lower than that in the control group (p<0.01). Note: *: p<0.05.

Effect of Endostatin on Proliferation Ability of A431 Cells

After endostatin treatment, as shown in Table II, there was no significant difference in OD values (450) at 24 h between the observation group and the control group (p>0.05). After 24 h, at each time point, OD values of the observation group were significantly lower than those of the control group (p<0.05) at each time point; the OD values (450) in both groups were increased with prolonged time. The CCK-8 proliferation curve is shown in Figure 2.

Table II. CCK-8 assay for detection of proliferation activity OD values in each group.

Culture time (h)	Observation group	Control group	t	p
12	0.44±0.11	0.41±0.08	0.66	0.52
24	0.99±0.14*#	1.21±0.15#	3.22	0.00
48	1.37±0.22*#	1.81±0.24#	4.05	0.00
72	1.59±0.22*#	2.09±0.21#	4.93	0.00
96	1.67±0.21*	2.34±0.23#	6.45	0.00
F	66.67	146.9		
p	0.00	0.00		

Note: *: at the same time point, compared with the control group, all p<0.05. #: in the same group, compared with the previous time point, p<0.05.

Effect of Endostatin on Invasion Ability of A431 Cells

After endostatin treatment, transwell experiment showed that the number of invading cells in the observation group and the control group were (38.25±8.13) and (98.25±9.14), respectively. The number of invading cells in the observation group was significantly smaller than that in the control group (p<0.01) (see Figure 3 for details).

Effect of Endostatin on Expression of EMT Related Markers in A431 Cells

The relative expression level of E-cadherin protein in the observation group was (0.34±0.03), which was significantly higher than that in the control group (0.14±0.01). The relative expression levels of N-cadherin protein in the observation and control groups were (0.18±0.05) and (0.43±0.03), respectively, and the expression level of N-cadherin protein in the observation group was significantly lower than that in the control group (all p<0.05). The relative expression levels of Vimentin protein in the observation group and control group were (0.23±0.08) and (0.56±0.12), respectively. The expression level of Vimentin protein in the observation group was significantly lower than that in the control group (p<0.05). The

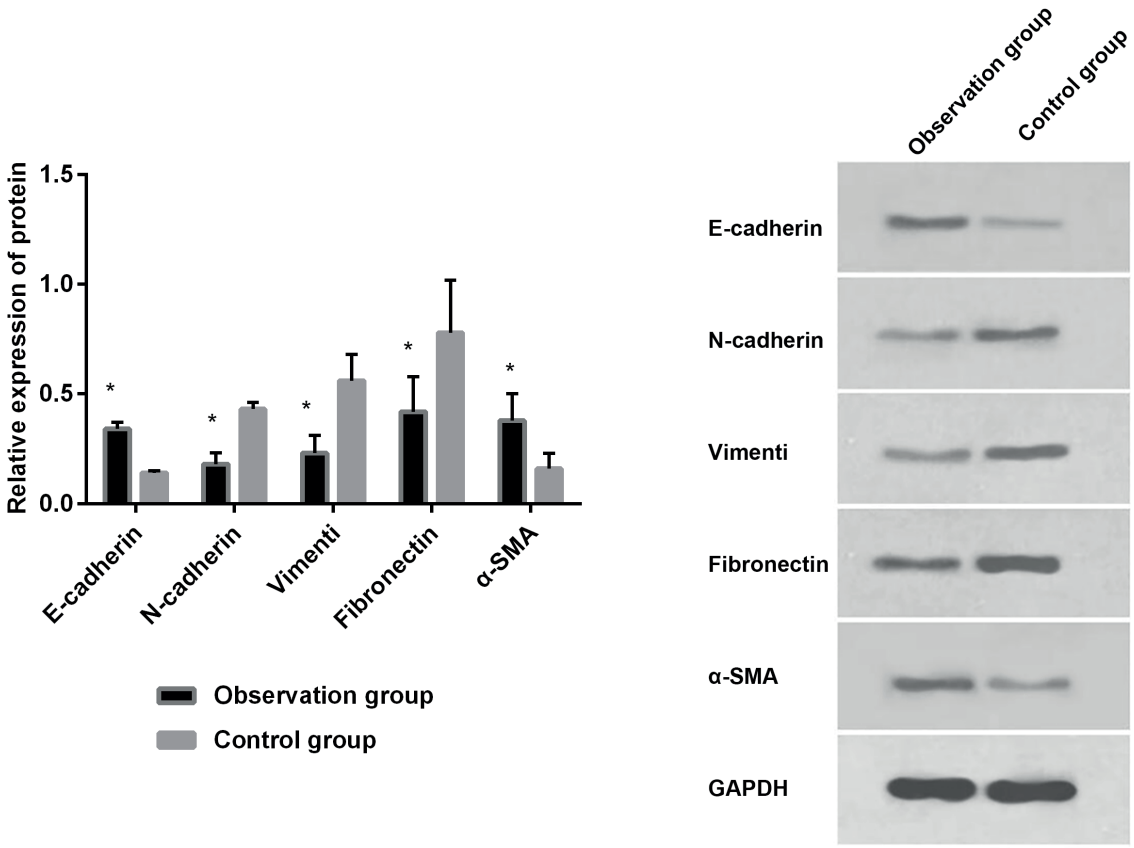

Figure 4. Effect of endostatin on expressions of E-cadherin and N-cadherin in A431 cells. The relative expression of E-cadherin protein in the observation group was significantly higher than that in the control group, and that of N-cadherin protein in the observation group was significantly lower than that in the control group. The relative expression level of Vimentin protein in the observation group was significantly lower than that in the control group ($p<0.05$). The relative expression level of Fibronectin protein in the observation group was significantly lower than that in the control group ($p<0.05$). The relative expression level of SMA protein was significantly higher than that of the control group ($p<0.05$), (all $p<0.05$). Note: *: in E-cadherin protein, compared with the control group, all $p<0.05$. #: in N-cadherin protein, compared with the control group, $p<0.05$. n=3.

relative expression level of Fibronectin protein in the observation group was (0.42±0.16), which was significantly lower than that in the control group (0.78±0.24) ($p<0.05$). The relative expression levels of α-SMA protein in the observation and control groups were (0.38±0.12) and (0.16±0.07), respectively. The relative expression of α-SMA protein in the observation group was significantly higher than that in the control group ($p<0.05$) (see Figures 4 and 5 for details).

Effects of Endostatin on Tumor Formation in Mouse Xenograft Model

No significant differences in tumor volume among the three groups at day 0 ($p>0.05$). Differences begin to show up on day 3. Tumor volume of the three groups increased with prolonged time (Figure 6). Tumor volume in the ES1 and ES2 group was smaller than that in the control group at each time point. After day 6, tumor volume in ES2 group was smaller than that in the ES1 group ($p<0.05$). The average tumor weight of ES1 group and ES2 group was lower than that of the control group, and the average tumor weight of ES2 group was lower than that of ES1 group ($p<0.05$) (see Figure 7 for details).

Discussion

As a chronic progressive disease with a low metastasis rate, BCC is an invasive and destructive cancer that can spread to deep soft tissue and bone tissue after the necrosis in the center, resulting in invasive necrosis of the skin and severe damage to the function of the corresponding tis-

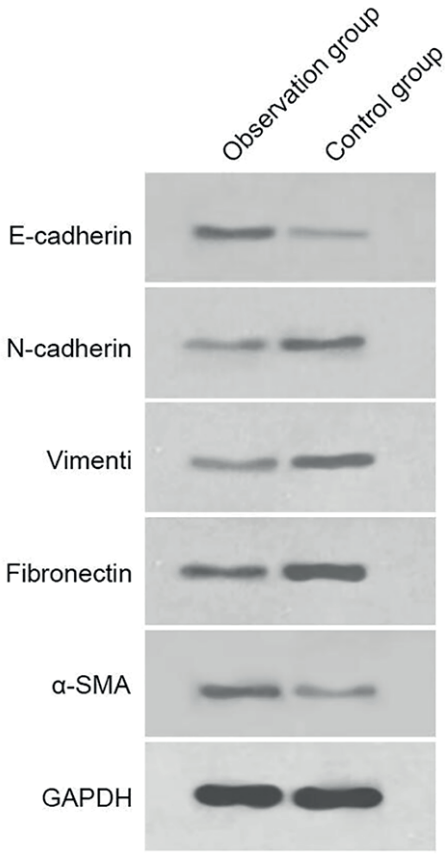

Figure 5. Detection of E-cadherin, N-cadherin, Vimentin, Fibronectin and a-SMA by Western blot.

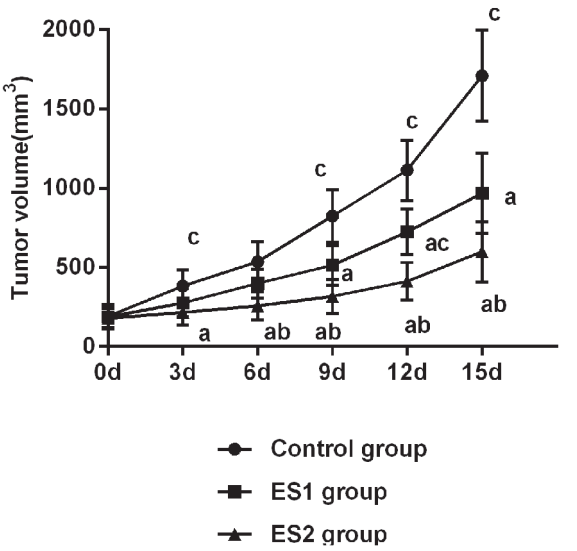

Figure 6. Comparison of tumor growth curve among the 3 groups. No significant differences in tumor volume among the three groups at day 0 ($p>0.05$). Differences begin to show up on day 3. Tumor volume of the three groups increased with prolonged time. Tumor volume in the ES1 and ES2 group was smaller than that in the control group at each time point. After day 6, tumor volume in ES2 group was always smaller than that in ES1 group ($p<0.05$). Note: a: compared with the control group at the same time point, $p<0.05$. b: compared with group ES1 at the same time point, $p<0.05$. c: compared with the previous time point in the same group, $p<0.05$.

sues. Once BCC metastasis occurs, the mortality rate will be extremely high[11,12]. Studies[13,14] have shown that the incidence of BCC in children and adolescents reveals an increasing trend. EMT refers to the fact that under certain pathological conditions, the tight junction between epithelial cells disappears to acquire the characteristics of wandering and migration like interstitial cells. EMT-inducing tumor cells can migrate through the basement membrane to adjacent tissues or even distant organs, so EMT is a necessary condition for the invasion and metastasis of tumor cells[15]. E-cadherin protein, N-cadherin protein, Vimentin protein, fibronectin and α-SMA protein are molecular biomarkers of EMT. E-cadherin and α-SMA proteins play an important role in cell junction and are epithelial marker proteins[16]. N-cadherin, Vimentin and Fibronectin are mesenchymal markers that contribute to cellular motility[17]. Studies[18,19] have shown that the expression of E-cadherin and α-SMA protein is down-regulated in EMT, and the expression of N-cadherin Vimentin protein and fibronectin is up-regulated. Chen et al18 found that endostatin could reverse EMT in esophageal cancer. The proliferation and invasion of solid tumor cells depend on the angiogenesis[19], which can be inhibited by endostatin. Therefore, this work investigated the effect of endostatin on the proliferation, migration, invasion and EMT of A431 cells, to understand the role of it in BCC and provide new suggestions for the treatment of it.

After endostatin treatment, the OD values detected by CCK-8 in the observation group were significantly lower than those in the control group at each time point after 24 h, indicating that the cell proliferation ability of the observation group significantly decreased compared with that in the control group, and endostatin inhibited the proliferation of A431 cells. After endostatin treatment, the number of invasive cells in the observation group was significantly lower than that in the control group, indicating that endostatin inhibited the invasion ability of A431 cells. Byekova et al[20] investigated the effect of endostatin on the resistance genes mdr 1 and gst-π of A431 cells and found that endostatin could inhibit the proliferation of A431, down-regulate expression of mdr 1

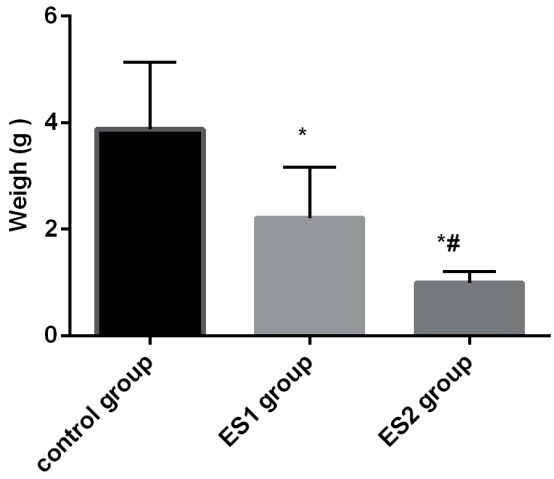

Figure 7. The average tumor weight of ES1 group and ES2 group was lower than that of the control group, and the average tumor weight of ES2 group was lower than that of the ES1 group ($p<0.05$). Group ES2 was significantly higher than group ES1 ($p<0.05$). Note: *: compared with the control group, $p<0.05$. #: compared with group ES1, $p<0.05$.

and gst-π, and increase the sensitivity of cancer cells to chemotherapy. Huang et al[21] found that endostatin could inhibit the proliferation and invasion of gastric cancer cells. This is consistent with the results of this study. After endostatin treatment, the relative expression levels of E-cadherin protein in the observation group was significantly higher than that in the control group, but the expression level of N-cadherin protein in the observation group was significantly lower than that in the control group, suggesting that endostatin could inhibit the N-cadherin expression and promote the E-cadherin expression in A431 cells, to reverse EMT.

In this work, we determined the concentration and action time of endostatin IC50. It was found that the proliferation inhibition of endostatin on A431 was closely related to the concentration and action time. According to the calculated IC50 at 24 h, 48 h and 72 h, the minimum concentration of IC50 and its corresponding action time were used in subsequent experiments. It can be seen from Table I that the inhibition rate of 40 μl/mg treatment for 72 h in the observation group was (46.72±2.98), close to 50%. However, this work also has some deficiencies. The specific pathway and mechanism involved in the endostatin-mediated regulation of the proliferation, invasion and EMT inhibition of A431 cells remain to be studied.

Conclusions

We found that endostatin can inhibit the proliferation, invasion and EMT of BCC cells. Our study provided new insights to the treatment of BCC.

Conflict of Interest

The Authors declare that they have no conflict of interest.

References

1) Ramachandran S, Fryer AA, Smith AG, Lear JT, Bowers B, Hartland AJ, Whiteside JR, Jones PW, Strange RC. Basal cell carcinomas: association of allelic variants with a high-risk subgroup of patients with the multiple presentation phenotype. Pharmacogenetics 2001; 11: 247-254.
2) Sterry W, Ruzicka T, Herrera E, Takwale A, Bichel J, Andres K, Ding L, Thissen MR. Imiquimod 5% cream for the treatment of superficial and nodular basal cell carcinoma: randomized studies comparing low-frequency dosing with and without occlusion. Br J Dermatol 2002; 147: 1227-1236.
3) Dummer R, Urosevic M, Kempf W, Hoek K, Hafner J, Burg G. Imiquimod in basal cell carcinoma: how does it work? Br J Dermatol 2003; 149 Suppl 66: 57-58.
4) Dokianakis DN, Koumantaki E, Billiri K, Spandidos DA. P53 codon 72 polymorphism as a risk factor in the development of HPV-associated non-melanoma skin cancers in immunocompetent hosts. Int J Mol Med 2000; 5: 405-409.
5) Sand M, Hessam S, Amur S, Skrygan M, Bromba M, Stockfleth E, Gambichler T, Bechara FG. Expression of oncogenic miR-17-92 and tumor suppressive miR-143-145 clusters in basal cell carcinoma and cutaneous squamous cell carcinoma. J Dermatol Sci 2017; 86: 142-148.
6) Verkouteren JAC, Ramdas KHR, Wakkee M, Nijsten T. Epidemiology of basal cell carcinoma: scholarly review. Br J Dermatol 2017; 177: 359-372.
7) Orlandi A, Bianchi L, Costanzo A, Campione E, Giusto Spagnoli L, Chimenti S. Evidence of increased apoptosis and reduced proliferation in basal cell carcinomas treated with tazarotene. J Invest Dermatol 2004; 122: 1037-1041.
8) Li VW, Li WW. Antiangiogenesis in the treatment of skin cancer. J Drugs Dermatol 2008; 7: s17-24.
9) Kurschat P, Eming S, Nashan D, Krieg T, Mauch C. Early increase in serum levels of the angiogenesis-inhibitor endostatin and of basic fibroblast growth factor in melanoma patients during disease progression. Br J Dermatol 2007; 156: 653-658.
10) Siemann DW. Therapeutic strategies that selectively target and disrupt established tumor vasculature. Hematol Oncol Clin North Am 2004; 18: 1023-1037.

11) Chang J, Zhu GA, Cheung C, Li S, Kim J, Chang AL. Association between programmed death ligand 1 expression in patients with basal cell carcinomas and the number of treatment modalities. JAMA Dermatol 2017; 153: 285-290.

12) Iftimia N, Yelamos O, Chen CJ, Maguluri G, Cordova MA, Sahu A, Park J, Fox W, Alessi-Fox C, Rajadhyaksha M. Handheld optical coherence tomography-reflectance confocal microscopy probe for detection of basal cell carcinoma and delineation of margins. J Biomed Opt 2017; 22: 76006.

13) Zhou W, Chen Z, Yang S, Xing D. Optical biopsy approach to basal cell carcinoma and melanoma based on all-optically integrated photoacoustic and optical coherence tomography. Opt Lett 2017; 42: 2145-2148.

14) Casari A, Argenziano G, Moscarella E, Lallas A, Longo C. Confocal and dermoscopic features of basal cell carcinoma in Gorlin-Goltz syndrome: a case report. Australas J Dermatol 2017; 58: e48-e50.

15) Liu W, Zhang B, Xu N, Wang MJ, Liu Q. miR-326 regulates EMT and metastasis of endometrial cancer through targeting TWIST1. Eur Rev Med Pharmacol Sci 2017; 21: 3787-3793

16) Chen F, Liu X, Cheng Q, Zhu S, Bai J, Zheng J. RUNX3 regulates renal cell carcinoma metastasis via targeting miR-6780a-5p/E-cadherin/EMT signaling axis. Oncotarget 2017; 8: 101042-101056.

17) Chen L, Munoz-Antonia T, Cress WD. Trim28 contributes to EMT via regulation of E-cadherin and N-cadherin in lung cancer cell lines. PLoS One 2014; 9: e101040.

18) Chen X, Zhang H, Zhu H, Yang X, Yang Y, Yang Y, Min H, Chen G, Liu J, Lu J, Cheng H, Sun X. Endostatin combined with radiotherapy suppresses vasculogenic mimicry formation through inhibition of epithelial-mesenchymal transition in esophageal cancer. Tumour Biol 2016; 37: 4679-4688.

19) Feldman AL, Pak H, Yang JC, Alexander HR, Jr., Libutti SK. Serum endostatin levels are elevated in patients with soft tissue sarcoma. Cancer 2001; 91: 1525-1529.

20) Byekova YA, Herrmann JL, Xu J, Elmets CA, Athar M. Liver kinase B1 (LKB1) in the pathogenesis of UVB-induced murine basal cell carcinoma. Arch Biochem Biophys 2011; 508: 204-211.

21) Huang G, Chen L: Recombinant human endostatin improves anti-tumor efficacy of paclitaxel by normalizing tumor vasculature in Lewis lung carcinoma. J Cancer Res Clin Oncol 2010; 136: 1201-1211.